CHIN. PHYS. LETT. Vol. 36, No. 3 (2019) 038701

An Improvement on the Combination of Magnetic Trap and Fluorescent Resonant Energy Transfer *

Da-guan Nong(农大官)[1,2], Ming Li(李明)[1,2]**

[1] *Beijing National Laboratory for Condensed Matter Physics, Institute of Physics, Chinese Academy of Sciences, Beijing 100190*

[2] *University of Chinese Academy of Sciences, Beijing 100049*

(Received 15 October 2018)

The combination of magnetic trap (MT) and fluorescence resonant energy transfer (FRET) allows for nanoscale measurements of configurational changes of biomolecules under force. However, the magnetic bead involved in MT experiments introduces a substantial amount of background fluorescence which reduces the signal-to-noise ratio (SNR) of FRET significantly. Moreover, the short lifetime of the dye used in FRET limits the total sampling time when combined with MT. Here we use a moveable tube lens to adjust the wave front in the light pathway of MT so that both images of the magnetic bead and the fluorescent signals can be detected when long DNA handles are used to reduce the auto-fluorescence of the magnetic bead. We utilize the internal trigger of an electron multiplying charge-coupled device camera to control a shutter so that the dye can be excited intermittently when long time measurement of FRET is needed. As a demonstration of the hybrid technique, we observe the unfolding/refolding dynamics of a DNA hairpin and measure the DNA unwinding activity of the saccharomyces cerevisiae Pif1 (Pif1). Our results show that the unwinding burst of Pif1 under external force is different from that without the force. In addition, the improvement provides a better SNR and a longer sampling time in experiments in the MT-FRET assay.

PACS: 87.80.Nj, 87.80.Fe, 82.37.Rs DOI: 10.1088/0256-307X/36/3/038701

Force plays a crucial role in many biological processes, such as modulating enzymatic activity and altering the kinetics of molecular bonds.[1,2] Force spectroscopy methods based on single-molecule manipulation have enabled researchers to observe biological processes in real time with unprecedented accuracy. However, solely single-molecule manipulation techniques probe only molecular end-to-end extension. Crucial details, such as the internal conformational changes of a protein, are not directly measured by these techniques. To overcome the limitation, researchers combined manipulation techniques with fluorescence microscopy, allowing more detailed measurement in force-dependent biological processes.[3,4] Among the mainstream manipulation methods, magnetic trap (MT) generates forces up to ∼200 pN by remotely exerting loads on multiple paramagnetic beads simultaneously.[5] In addition to force range advantages, MT avoids trap-induced photo-damage and is capable of high-throughput measurement when combined with fluorescence microscopy.

The combination of MT and fluorescence imaging provides a simultaneous measurement of the conformational changes of a protein and its function.[6–8] However, the auto-fluorescence of the magnetic bead (Fig. 2(a)) reduces the SNR significantly in single-molecule fluorescence imaging.[4,9] Moreover, in typical fluorescence imaging, the lifetime of most fluorophores is ∼10 s before photo-bleaching and can be prolonged by ∼10 fold using oxygen scavenging systems.[10] The short lifetime limits the total sampling time of the hybrid technique. To overcome these limitations, we used a long DNA linker to spatially separate the magnetic bead from the fluorescent dyes to reduce the background. To ensure that both of the images of the magnetic bead and the fluorescence dye can be detected, we used a moveable tube lens to adjust the wave front in the light pathway of MT. We used the internal trigger of an electron multiplying charge-coupled device camera (EMCCD) to control a shutter so that the fluorescence dye can be excited intermittently. The lifetime of the dye can thus be prolonged 2 fold at a duty cycle of 50% or longer by adjusting the duty cycle of the trigger signal. With the improvements we made on this hybrid technique, we first demonstrated the unfolding/folding dynamics of a DNA hairpin under the application of force and then presented the measurement of the Pif1 unwinding dynamics under external forces.

The experimental system that we built was based on an inverted microscope. The configuration is illustrated in Fig. 1. The optical layout of the instrument consists of an MT light pathway (brownish red) and a two-color smFRET light pathway (green, red, yellow). The magnetic bead (M-270, Invitrogen) is illuminated by an infrared LED light source (850 nm, LEDC49, Thorlabs) and detected by a charge-coupled device camera (Guppy GE680, Prosilica). A translation stage (MP285, Sutter Instrument) is utilized to control the position of the magnets and a piezo stage (P-733.3, Princeton Instruments) is utilized to control the position of the sample chamber. The excita-

*Supported by the National Natural Science Foundation of China under Grant No 11574382.

**Corresponding author. Email: mingli@iphy.ac.cn

tion laser (532 nm, Sapphire 532-150cw, coherent) is guided to the sample through an oil-immersion objective (UAPON100x1.49TIRF, OLYMPUS). Cy3 and Cy5 signals are collected by the objective lens and guided to a high-sensitivity EMCCD (Ixon-897, Andor) after being separated and filtered by dichroic mirrors and band-pass filters (OptoSplit Ⅱ, Chroma). The internal trigger of an EMCCD is extracted to control the shutter (LCS-5, CNI Co., Ltd). Both of the images of the magnetic bead and the fluorescence dye are analyzed using homemade software.[11]

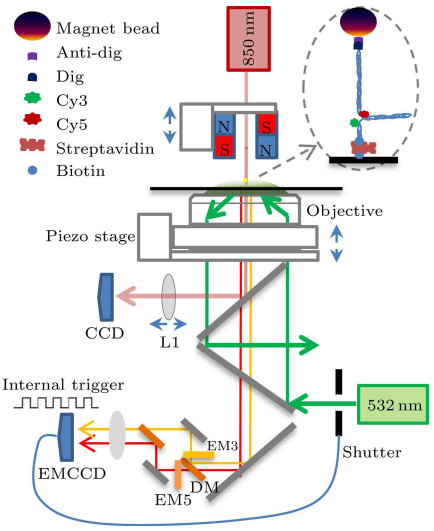

Fig. 1. Hybrid MT-smFRET microscopy setup.

The FRET efficiency is defined by $E = I_a/(I_a+I_d)$. I_a and I_d are the fluorescent intensities of the accepter (Cy5) and donor (Cy3), respectively. In this study, Cy3 and Cy5 signals are separated and filtered by a dichroic mirror (Fig. 1, DM, T647lpxr, Chroma) and two band-pass filters (Fig. 1, EM3, EM5, ET580/40, T670/50, Chroma) and then guided to different areas in the EMCCD. According to different filter sets, there is leakage of photons from the donor to the accepter channel due to the spectral overlap between the dyes. The leakage should be measured and taken into account in the calculation of transfer efficiency. We excited the sample labeled by Cy3 until photo-bleaching was observed (Fig. 3(b)), the leakage was then calculated by leakage $= I_a/(I_a + I_d)$ and it is about 7.6% in the case of our filter sets.

In contrast with the single-molecule fluorescence signal, the magnetic bead is a fluorescent cluster consisting of hundreds of molecules. It introduces a substantial amount of background fluorescence which reduces SNR in the single-molecule fluorescence imaging. Figure 2(a) shows typical images of the Cy3 fluorescence dye and magnetic bead at the different DNA extensions under 532 nm laser excitation. The Cy3 signal is almost hidden in the background fluorescence of the bead when the DNA extension $d = 1\,\mu m$ (Fig. 2(a), left). As shown in Fig. 2(a), the intensity of the auto-fluorescence decreases as the bead is pulled away from the glass-buffer surface. However, the single-molecule fluorescence imaging needs a precise focus on the glass surface. Thus the bead at $\sim$3 µm above the dye is severely defocused, making it difficult to track (Fig. 2(a), right).

To address this problem, we adjusted the wave front in the light pathway of MT by changing the position of the imaging lens (Fig. 1, L1) before tracking the magnetic bead. Figure 2 shows the diffraction pattern of a magnetic bead connected by a DNA of a contour length of $\sim 3\,\mu m$ before (Fig. 2(a), right) and after the adjustment of L1 (Fig. 2(b)). The adjustment of L1 makes it possible to track the bead with a longer linker DNA for a better SNR in the fluorescence imaging (Fig. 2(a), right).

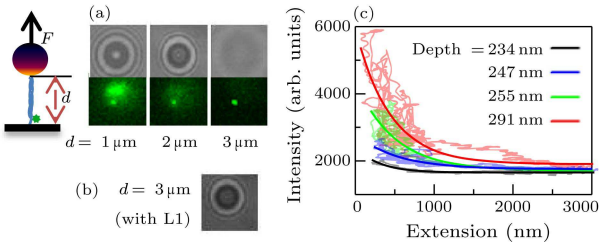

Fig. 2. Auto-fluorescence of the magnetic bead. (a) Images of the Cy3 fluorescence dye and diffraction patterns of the magnetic bead at the different DNA extensions under 532 nm laser excitation. The images of Cy3 are interfered by the auto-fluorescence of the bead with a short DNA linker (left and middle). A longer DNA linker decreases the auto-fluorescence. However, the severe defocusing makes it difficult to track the bead (right). (b) The adjustment of L1 improves the diffraction pattern of magnetic bead with long DNA linker. (c) Auto-fluorescence decreases exponentially with distance of the bead away from the surface at different penetration depths.

It is noted that the intensity of the auto-fluorescence decreases as the bead is pulled away from the glass-buffer surface. Thus by measuring the intensity and combining it with the information of DNA extension measured by MT, we obtained the intensity of auto-fluorescence as a function of DNA extension. The penetration depth of TIRF was then calculated by a single exponential fitting of the curve of intensity to distance (Fig. 2(c)). To minimize the background fluorescence, we chose a minimum penetration depth at about 180 nm.

Photo-bleaching is an important feature in single-molecule fluorescence imaging. Fluorescent molecules will eventually be destroyed by the excitation light (Fig. 3(b)). In most cases, the lifetime of fluorescent molecules is $\sim$100 s with optimization of imaging parameters.[10] However, due to the unstable immobilization of magnetic bead, the sampling time of MT is usually $\sim$10 min or longer. Thus the lifetime of the dye limits the total sampling time of the hybrid technique. To address this problem, we utilized a shutter to switch the excitation laser on and off so that the fluorescence dye can be excited intermittently to obtain a longer sampling time of FRET. The shutter is controlled by the internal trigger of the EMCCD, i.e.,

switched on during exposures and off between them (Fig. 3(a)). The duty cycle of the internal trigger is programmable via the software. After the improvement, the lifetime of dyes can be prolonged ∼2 fold at duty cycle of 50% (Fig. 3(d)). We fixed the time of exposure and increased the interval time so that the intermittent excitation will not reduce the SNR. However, the temporal resolution decreases since we skipped part of the reaction. Therefore, this improvement is applicable mainly to slow-reaction biological processes.

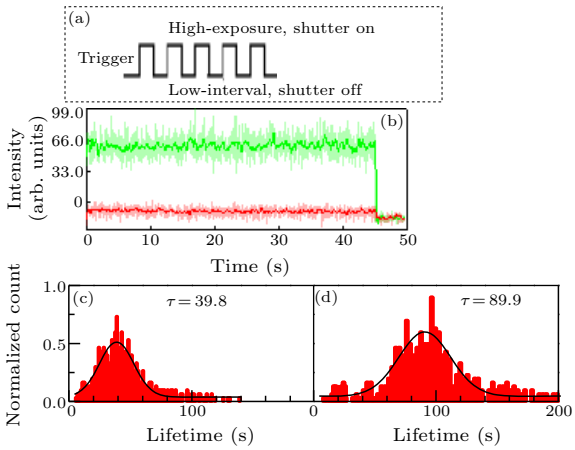

Fig. 3. Scheme of the intermittent excitation. (a) Internal trigger of EMCCD. (b) Photo-bleaching of fluorescent molecules. (c) Lifetime of dyes at continuous excitation and (d) 50% duty cycle of intermittent excitation.

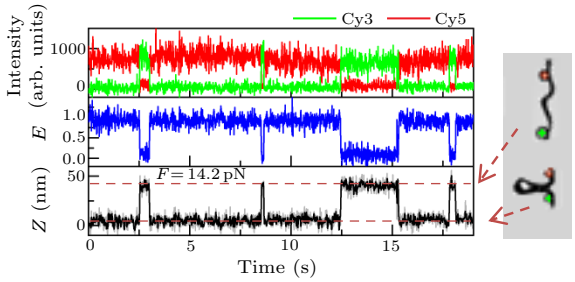

Fig. 4. Unfolding/refolding dynamics of a DNA hairpin. The intensity time traces of Cy3 (green) and Cy5 (red), together with the length information of the magnetic bead (black) at 14.2 pN.

As a demonstration of the hybrid technique, we studied the force-induced unfolding/refolding dynamics of a DNA hairpin with a 40-bp stem and a 4-nt loop. The DNA construct is labeled with Cy3 and Cy5. To exert a force on the hairpin, the DNA hairpin is immobilized onto a glass surface and attached to a magnetic bead via a 2600-bp linker DNA (Fig. 1). The FRET efficiency and the tracking of magnetic bead report the unfolding/refolding of hairpin synchronously. Figure 5 shows representative fluorescence intensity time traces at 14.2 pN for Cy3 and Cy5, together with the FRET efficiency calculated from the same data set and the tracking information of the magnetic bead. The result demonstrates that we have successfully combined MT with smFRET.

Pif1 belongs to the SF1 superfamily of helicases,[12] it is a 5′–3′ helicase and plays an important role in the maintenance of both mitochondrial and nuclear genome stabilities.[13,14] Previous studies in Pif1-catalyzed DNA unwinding have shown that Pif1 is a force-regulated helicase.[15] The load of force enhances the unwinding rate and the total unwinding length of Pif1 significantly. We have designed an experiment to demonstrate the measurement of Pif1-catalyzed DNA unwinding dynamics under external force. The experimental scheme is illustrated in Fig. 5(a). Cy3 and Cy5 were labeled at the junction. The substrate was constructed with a 26-nt single-stranded gap for the binding of Pif1. The Pif1 concentration during pre-incubation with the DNA substrates was 5 nM.

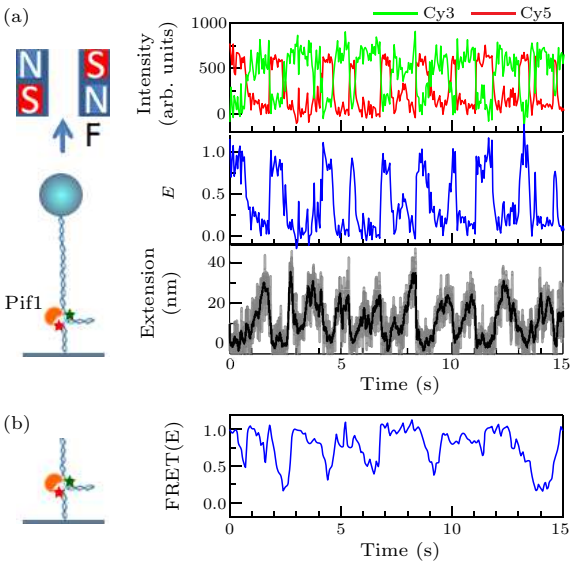

Fig. 5. Pif1-catalyzed DNA unwinding with MT-FRET and conventional smFRET. (a) The intensity time traces of Cy3 (green) and Cy5 (red) together with the unwinding bursts of the magnetic bead (black) at 4.2 pN and 20 μM ATP. (b) A typical time trace obtained with the conventional smFRET.

The unwinding traces of MT (Fig. 5(a), black) showed simple saw-tooth patterns with repeated unwinding bursts, which is consistent with previous studies.[15] The representative fluorescence intensity time traces of Cy3 and Cy5, together with FRET efficiency calculated from the same data in Fig. 5(b) (green, red and blue) show the same patterns of unwinding bursts. Note that FRET efficiency from 0 to 1 represents ∼10 nm change in DNA extension. Thus SNR of smFRET is better than that of MT. By contrast, Figure 5(b) shows similar unwinding bursts measured with a conventional FRET setup at the same concentration of ATP. Without the force, the unwinding length is shorter and the unwinding rate is lower.

Numerous techniques have been developed to study protein-DNA interactions at single molecule level. However, direct measurements of the relation between the protein conformational changes and its

function are rare. In this study, we develop a technique to combine MT with FRET to address this problem. We made improvements on the instrument to increase SNR and prolong the sampling time of FRET when combined with MT. After these improvements, we demonstrate the unfolding/refolding dynamics of DNA hairpin under the application of force and then present the measurement of the Pif1 unwinding dynamics under external force. The results reveal that the unwinding bursts of Pif1 under an external force is different from that without the force. MT-FRET is a promising hybrid technique for single-molecule studies where both force and fluorescent signals are required.

References

[1] Cecconi C, Shank E A, Bustamante C and Marqusee S 2005 *Science* **309** 2057
[2] Marshall B T, Long M, Piper J W, Yago T, McEver R P and Zhu C 2003 *Nature* **423** 190
[3] Li C and Li J 2015 *Chin. Phys. Lett.* **32** 108702
[4] Cordova J C, Das D K, Manning H W and Lang M J 2014 *Curr. Opin. Struct. Biol.* **28** 142
[5] Lipfert J, Hao X M and Dekker N H 2009 *Biophys. J.* **96** 5040
[6] Graves E T, Duboc C, Fan J, Stransky F, Leroux C M and Strick T R 2015 *Nat. Struct. Mol. Biol.* **22** 452
[7] Wang S, Zheng H Z, Zhao Z Y, Lu Y and Xu C H 2013 *Acta Phys. Sin.* **62** 168703 (in Chinese)
[8] Zhao Z Y, Xu C H, Li J H, Huang X Y, Ma J B and Lu Y 2017 *Acta Phys. Sin.* **66** 188701 (in Chinese)
[9] Capitanio M and Pavone F S 2013 *Biophys. J.* **105** 1293
[10] Roy R, Hohng S and Ha T 2008 *Nat. Methods* **5** 507
[11] Gosse C and Croquette V 2002 *Biophys. J.* **82** 3314
[12] Tran P L T, Pohl T J, Chen C F, Chan A, Pott S and Zakian V A 2017 *Nat. Commun.* **8** 15025
[13] Paeschke K, Bochman M L, Garcia P T, Cejka P, Friedman K L, Kowalczykowski S C and Zakian V A 2013 *Nature* **497** 458
[14] Boulé J B and Zakian V A 2007 *Nucl. Acids Res.* **35** 5809
[15] Li J H, Lin W X, Zhang B, Nong D G, Ju H P, Ma J B, Xu C H, Ye F F, Xi X G, Li M, Lu Y, Dou S X 2016 *Nucl. Acids Res.* **44** 4330